

# Path Selection and Rate Allocation in Self-Backhauled mmWave Networks

Trung Kien Vu\*, Chen-Feng Liu\*, Mehdi Bennis\*, Mérouane Debbah<sup>†‡</sup>, and Matti Latva-aho\*

\*Centre for Wireless Communications, University of Oulu, Finland

<sup>†</sup>Mathematical and Algorithmic Sciences Lab, Huawei France R&D, Paris, France

<sup>‡</sup>CentraleSupélec, Université Paris-Saclay, Gif-sur-Yvette, France

E-mail: {trungkien.vu, chen-feng.liu, mehdi.bennis, matti.latva-aho}@oulu.fi, merouane.debbah@huawei.com

**Abstract**—We investigate the problem of multi-hop scheduling in self-backhauled millimeter wave (mmWave) networks. Owing to the high path loss and blockage of mmWave links, multi-hop paths/routes between the macro base station and the intended users via full-duplex small cells need to be carefully selected. This paper addresses the fundamental question: “how to select the best paths and how to allocate rates over these paths subject to latency constraints?” To answer this question, we propose a new system design, which factors in mmWave-specific channel variations and network dynamics. The problem is cast as a network utility maximization subject to a bounded delay constraint and network stability. The studied problem is decoupled into: (i) a path/route selection and (ii) rate allocation, whereby learning the best paths is done by means of a reinforcement learning algorithm, and the rate allocation is solved by applying the successive convex approximation method. Via numerical results, our approach ensures reliable communication with a guaranteed probability of 99.9999%, and reduces latency by 50.64% and 92.9% as compared to baselines.

**Keywords**—URLLC, low latency, reliable communication, mmWave communications, multi-hop scheduling, ultra dense small cells, stochastic optimization, reinforcement learning, non-convex optimization.

## I. INTRODUCTION

The fifth generation (5G) networks are required to support high data rates of multiple gigabits per second (Gbps) and to have 50 billion connected devices by 2020 [1]. In parallel to that, due to the current scarcity of wireless spectrum, both academia and industry have paid attention to the underutilized frequency bands (30-300 GHz) [1], [2]. The required capacity increase can be achieved by (i) advanced spectral-efficient transmission techniques, e.g., massive multiple-input multiple-output (MIMO); and (ii) ultra-dense self-backhauled small cell deployments [3], [4]. Although mmWave frequency bands offer huge bandwidth, operating at higher frequency bands experiences high propagation attenuation [2], which requires smart beamforming to achieve highly directional gains. Owing to the short wavelength, mmWave frequency bands enable packing a massive number of antennas into highly directional beamforming over a short distance as compared to the conventional frequency bands [2]. Besides that, mmWave communication requires higher transmit power and is very sensitive to blockage, when transmitting over a long distance [2], [4]. Hence, instead of using a single hop [4], [5], a multi-hop self-backhauling architecture is a promising solution [6], [7].

Focusing on maximizing the quality of multimedia applications, the authors in [8] studied multi-hop routing for device-to-device communication. The work [9] studied the multi-hop relaying transmission challenges for mmWave systems. Therein, taking traffic dynamics and link qualities into account, [8], [9] aimed at maximizing the network throughput. In addition, path selection and multi-path congestion control was studied in [10] in which the aggregate utility is increased as more paths are provided.

Despite the interesting results of the aforementioned works, using multi-hop transmissions raises the issue of increased delay which has been generally ignored. Note that the issues of latency and reliability are two key components in 5G networks and beyond [11]. Moreover, splitting data into too many paths leads to increased signaling overhead and causes network congestion. Hence, there is a need for fast and efficient multi-hop multi-path scheduling with respect to traffic dynamics and channel fluctuations in self-backhauled mmWave networks. Our previous studies focused on single-hop ultra-reliable low latency communication (URLLC)-centric transmission in mmWave networks [5]. In this work, we further extend the previous work to the multi-hop multi-path wireless backhaul scenario and study a joint path selection and rate allocation problem. In summary, we address two fundamental aspects enabling multi-hop multi-path self-backhauled mmWave networks: (i) how to select the best paths while taking traffic dynamics and link qualities into account; (ii) how to capture elements of URLLC while maximizing the network utility.

### A. Main contribution

Considering a multi-hop multi-path self-backhauled mmWave network, we propose an efficient system design to support URLLC. In particular, our goal is to maximize a general network utility subject to network stability and the delay bound violation constraint with a tolerable probability (reliability). Leveraging Lyapunov stochastic optimization [12], the studied problem is decoupled into multi-hop path/route selection and rate allocation sub-problems. The challenging questions we seek to address are: (i) *over which paths should the traffic flow be forwarded?* and (ii) *what is the data rate per flow/sub-flow* while ensuring low-latency and ultra-reliability constraints? To answer these questions, we utilize *regret learning* techniques to exploit the benefits of the historical information which aids in selecting the best paths. For rate allocation, the corresponding mathematical

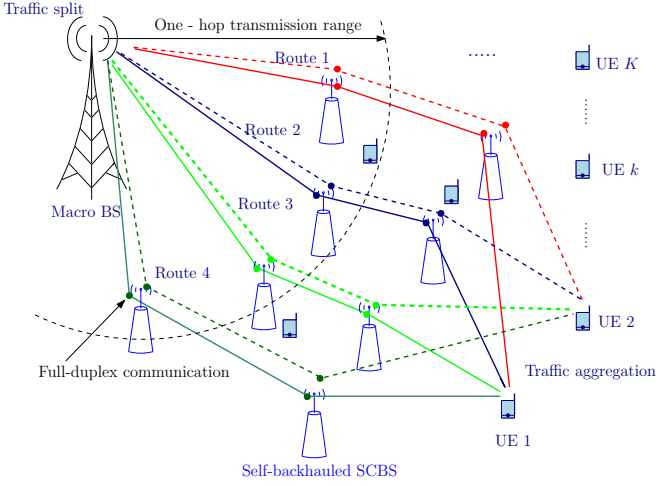


Fig. 1: 5G multi-hop self-backhauled mmWave networks.

problem belongs to a non-convex combinatorial program [13]. By exploiting the hidden convexity of the problem, we propose an iterative rate allocation algorithm based on the second-order cone program (SOCP) to obtain a local optimal of the approximated convex problem. Numerical results verify the effectiveness of the proposed path selection and rate allocation solution.

## II. SYSTEM MODEL

Let us consider a multi-hop multi-path heterogeneous cellular network (HCN) which consists of a macro base station (MBS), a set of  $B$  self-backhauled small cell base stations (SCBSs), and a set  $\mathcal{K}$  of UEs  $K$  single-antenna user equipments (UEs) as shown in Fig. 1. Let  $\mathcal{B} = \{0, 1, \dots, B\}$  denote the set of all base stations (BSs) in which index 0 refers to the MBS. We consider the downlink transmission in which the traffic is generated from the MBS to UEs via self-backhauled SCBSs. The in-band wireless backhaul is used to provide backhaul among BSs and a full-duplex transmission protocol is assumed at SCBSs with perfect self-interference cancellation [14]. Each BS is equipped with  $N_b$  transmitting antennas and we denote the propagation channel between BS  $b$  and UE  $k$  as  $\mathbf{h}_{(b,k)} = \sqrt{N_b} \mathbf{\Theta}_{(b,k)}^{1/2} \mathbf{w}_{(b,k)}$  [4], where  $\mathbf{\Theta}_{(b,k)} \in \mathbb{C}^{N_b \times N_b}$  depicts the antenna spatial correlation, and the elements of  $\mathbf{w}_{(b,k)} \in \mathbb{C}^{N_b \times 1}$  are independent and identically distributed (i.i.d.) with zero mean and variance  $1/N_b$ .

The network topology is modeled as a directed graph  $\mathcal{G} = (\mathcal{N}, \mathcal{L})$ , where  $\mathcal{N} = \mathcal{B} \cup \mathcal{K}$  represents the set of nodes including BSs and UEs.  $\mathcal{L} = \{(i, j) | i \in \mathcal{B}, j \in \mathcal{N}\}$  denotes the set of all directional edges  $(i, j)$  in which nodes  $i$  and  $j$  are the transmitter and the receiver, respectively.

We consider a (stochastic) queuing network operating in discrete time  $t \in \mathbb{Z}^+$  [12]. There are  $F$  independent data at the MBS. Each data traffic is destined for one UE, whereas one UE receives multiple data streams, i.e.,  $F \geq K$ . Hereafter, we refer to data traffic as data flow. We use  $\mathcal{F}$  to represent the set of  $F$  data flows. The MBS splits each flow  $f$  into multiple sub-flows which are sent through a set of disjoint paths. The traffic aggregation capability is assumed at the UEs [15].

We assume that there exists  $Z_f$  number of disjoint routes from the MBS to the UE for flow  $f$ . For any disjoint route  $m = \{1, \dots, Z_f\}$ , we denote  $\mathcal{Z}_f^m$  as the route state, which contains all route information such as topology and queue states for every hop. Let  $\mathcal{Z}_f = \{\mathcal{Z}_f^1, \dots, \mathcal{Z}_f^m, \dots, \mathcal{Z}_f^{Z_f}\}$  denote route states observed by flow  $f$ . We use the flow-split indicator vector  $\mathbf{z}_f = (z_f^1, \dots, z_f^{Z_f})$  to denote how the MBS splits flow  $f$ , where  $z_f^m = 1$  means path  $m$  is used to send data for flow  $f$ . Otherwise,  $z_f^m = 0$ . Let  $\mathcal{N}_i^{(o)}$  denote the set of the next hops from node  $i$  via a directional edge. We denote the next hop of flow  $f$  from BS  $b$  as  $b_f^{(o)}$ .

In addition,  $\mathbf{h} = (\mathbf{h}_{(i,j)} | (i, j) \in \mathcal{L})$  denotes the channel propagation vector, and we denote  $p_{(i,j)}^f$  as the transmit power of node  $i$  assigned to node  $j$  for flow  $f$  such that  $\sum_{f \in \mathcal{F}} \sum_{j \in \mathcal{N}_i^{(o)}} p_{(i,j)}^f \leq P_i^{\max}$ , where  $P_i^{\max}$  is the maximum transmit power of node  $i$ . We have the power constraint as

$$\mathcal{P} = \left\{ p_{(i,j)}^f \geq 0, i, j \in \mathcal{N}, \left| \sum_{f \in \mathcal{F}} \sum_{j \in \mathcal{N}_i^{(o)}} p_{(i,j)}^f \leq P_i^{\max} \right. \right\}. \quad (1)$$

Vector  $\mathbf{p} = (p_{(i,j)}^f | \forall i, j \in \mathcal{N}, \forall f \in \mathcal{F})$  denotes the transmit power over all flows. Therefore, for a given channel state and transmit power, the data rate in edge  $(i, j)$  over flow  $f$  can be posted as a function of channel state and transmit power, i.e.,  $R_{(i,j)}^f(\mathbf{h}, \mathbf{p})$ , such that  $\sum_{f \in \mathcal{F}} R_{(i,j)}^f = R_{(i,j)}$ . We denote  $\mathbf{R} = (R_{(i,j)}^f | \forall i, j \in \mathcal{N}, \forall f \in \mathcal{F})$  as a vector of data rates over all flows.

Let  $Q_b^f(t)$  denote the queue length at BS  $b$  at time slot  $t$  for flow  $f$ . The queue length evolution at the MBS  $b = 0$  is

$$Q_b^f(t+1) = \left[ Q_b^f(t) - \sum_{m=1, b_f^{(o)} \in \mathcal{Z}_f^m} z_f^m R_{(b, b_f^{(o)})}^f(t) \right]^+ + \mu^f(t). \quad (2)$$

where  $[\cdot]^+ = \max\{\cdot, 0\}$ , and  $\mu^f(t)$  is the data arrival at the MBS during slot  $t$ , which is i.i.d. over time with a mean value  $\bar{\mu}^f$ . Due to the disjoint paths, the incoming rate at the SCBS is either from one SCBS or the MBS, which is denoted as  $b^{(1)}$ . The queue evolution at the SCBS  $b = \{1, \dots, B\}$  is given by

$$Q_b^f(t+1) \leq \left[ Q_b^f(t) - R_{(b, b_f^{(o)})}^f(t) \right]^+ + R_{(b^{(1)}, b)}^f(t). \quad (3)$$

## III. PROBLEM FORMULATION

Assume that the MBS determines routes to split data flow  $f$  with a given probability distribution, i.e.,  $\pi_f = (\pi_f^1, \dots, \pi_f^{Z_f} | \pi_f^m = \Pr(z_f = z_f^m))$ . Here,  $\pi_f$  is the probability mass function (PMF) of the flow-split vector, i.e.,  $\sum_{m=1}^{Z_f} \pi_f^m = 1$ . We denote  $\pi = \{\pi_1, \dots, \pi_f, \dots, \pi_F\} \in \Pi$  as the global probability distribution of all flow-split vectors in which  $\Pi$  is the set of all possible global PMFs. Let  $\bar{x}_0^f$  denote the achievable average rate of flow  $f$ , where  $\bar{x}_0^f \triangleq \lim_{t \rightarrow \infty} \frac{1}{t} \sum_{\tau=1}^t x_0^f(\tau)$

and  $x_0^f(\tau) = \sum_{m=1, b_f^{(o)} \in \mathcal{Z}_f^m} \mathbb{E}[z_f^m R_{(b, b_f^{(o)})}^f(\tau)] | b = 0$ . We assume that the achievable rate is bounded, i.e.,

$$0 \leq x_0^f(t) \leq a_{\max}^f, \quad (4)$$

where  $a_{\max}^f$  is the maximum achievable rate of flow  $f$  at every time  $t$ . Vector  $\bar{\mathbf{x}} = (\bar{x}_0^1, \dots, \bar{x}_0^F)$  denotes the time average of rates over all flows. Let  $\mathcal{R}$  denote the rate region, which is defined as the convex hull of the average rates, i.e.,  $\bar{\mathbf{x}} \in \mathcal{R}$ .

We define  $U_0$  as a network utility function, i.e.,  $U_0(\bar{\mathbf{x}}) = \sum_{f \in \mathcal{F}} U(\bar{x}_0^f)$ . Here,  $U(\cdot)$  is assumed to be a twice differentiable, concave, and increasing  $L$ -Lipschitz function for all  $\bar{\mathbf{x}} \geq 0$ . According to Little's law [16], the queuing delay is defined as the ratio of the queue length to the average arrival rate. By taking account of the probabilistic delay constraints for each flow/subflow, the following network utility maximization (NUM) is formulated as:

$$\text{OP: } \max_{\boldsymbol{\pi}, \mathbf{x}, \mathbf{p}} U_0(\bar{\mathbf{x}}) \quad (5a)$$

$$\text{subject to } \Pr\left(\frac{Q_b^f(t)}{\bar{\mu}_f} \geq \beta\right) \leq \epsilon, \forall t, f \in \mathcal{F}, b \in \mathcal{B}, \quad (5b)$$

$$\lim_{t \rightarrow \infty} \frac{\mathbb{E}[|Q_b^f|]}{t} = 0, \forall f \in \mathcal{F}, \forall b \in \mathcal{B}, \quad (5c)$$

$$\mathbf{x}(t) \in \mathcal{R}, \quad (5d)$$

$$\boldsymbol{\pi} \in \Pi, \quad (5e)$$

and (1), (4),

where  $\Pr(\cdot)$  denotes the probability operator,  $\beta$  reflects the maximum allowed delay requirement for UEs, and  $\epsilon \ll 1$  is the target probability for reliable communication. The probabilistic delay constraint (5b) implies that the probability that the delay for each flow at node  $b$  is greater than  $\beta$  is very small, which captures the latency and reliability constraints. It is also used to avoid congestion for each flow  $f$  at any point (BS) in the network if the queue length is greater than  $\beta \bar{\mu}_f$ . More importantly, (5b) forces the transmission of all BSs, and (5c) maintains network stability.

We replace the non-linear constraint (5b) with a linear deterministic equivalent by applying Markov's inequality which gives  $\Pr(X \geq a) \leq \mathbb{E}[X]/a$  for a non-negative random variable  $X$  and  $a > 0$ . Thus, we relax (5b) as

$$\mathbb{E}[Q_b^f(t)] \leq \bar{\mu}_f \epsilon \beta. \quad (6)$$

Assuming that  $\mu^f(t)$  follows a Poisson arrival process, we derive the expected queue length in (2) for  $b = 0$  as

$$\mathbb{E}[Q_b^f(t)] = t \bar{\mu}_f - \sum_{\tau=1}^t \sum_{m=1, b_f^{(o)} \in \mathcal{Z}_f^m} \pi_f^m z_f^m R_{(b, b_f^{(o)})}^f(\tau), \quad (7)$$

and the expected queue length in (3) for each SCBS as

$$\mathbb{E}[Q_b^f(t)] = \sum_{\tau=1}^t \sum_m \pi_f^m z_f^m \left( R_{(b^{(1)}, b)}^f(\tau) - R_{(b, b_f^{(o)})}^f(\tau) \right). \quad (8)$$

Subsequently, combining the constraints (6) and (7), we obtain, for MBS  $b = 0$ ,

$$\begin{aligned} \bar{\mu}_f(t - \epsilon \beta) - \sum_{\tau=1}^{t-1} \sum_{m=1, b_f^{(o)} \in \mathcal{Z}_f^m} \pi_f^m z_f^m R_{(b, b_f^{(o)})}^f(\tau) \\ \leq \sum_{m=1, b_f^{(o)} \in \mathcal{Z}_f^m} \pi_f^m z_f^m R_{(b, b_f^{(o)})}^f(t). \end{aligned} \quad (9)$$

$$\begin{aligned} \text{Similarly, for each SCBS } b = \{1, \dots, B\}, \text{ we have} \\ -\bar{\mu}_f \epsilon \beta + \sum_{\tau=1}^t \sum_m \pi_f^m z_f^m \left( R_{(b^{(1)}, b)}^f(\tau) - R_{(b, b_f^{(o)})}^f(\tau) \right) \\ \leq \sum_m \pi_f^m z_f^m \left( R_{(b, b_f^{(o)})}^f(t) - R_{(b^{(1)}, b)}^f(t) \right), \end{aligned} \quad (10)$$

by combining (6) and (8). With the aid of the above derivations, we consider (9) and (10) instead of (5b) in the original problem (5). In practice, since the statistical information of all candidate paths to decide  $\pi_f, \forall f \in \mathcal{F}$ , is not available beforehand, solving (5) is very difficult. One solution is that paths are randomly assigned to each flow which does not guarantee optimality, whereas applying an exhaustive search is not practical. Therefore, in this work, we propose a low-complexity approach by invoking tools from Lyapunov stochastic optimization which achieves the optimal performance without requiring the statistical information beforehand.

#### IV. PROPOSED ALGORITHM

Let us start by rewriting (5) equivalently as [12]

$$\text{RP: } \max_{\bar{\boldsymbol{\varphi}}, \boldsymbol{\pi}, \mathbf{p}} U_0(\bar{\boldsymbol{\varphi}}) \quad (11a)$$

$$\text{subject to } \bar{\varphi}_0^f - \bar{x}_0^f \leq 0, \forall f \in \mathcal{F}, \quad (11b)$$

(1), (4), (5c), (5e), (9), (10),

where the new constraint (11b) is introduced to replace the rate constraint (5d) with new auxiliary variables  $\bar{\boldsymbol{\varphi}} = (\bar{\varphi}_0^1, \dots, \bar{\varphi}_0^F)$ . In (11b),  $\bar{\varphi} \triangleq \lim_{t \rightarrow \infty} \frac{1}{t} \sum_{\tau=1}^t \mathbb{E}[|\varphi(\tau)|]$ . In order to ensure the inequality constraint (11b), we introduce a virtual queue vector  $Y_0^f(t)$ , which is given by

$$Y_0^f(t+1) = \left[ Y_0^f(t) + \varphi_0^f(t) - x_0^f(t) \right]^+, \forall f \in \mathcal{F}. \quad (12)$$

Let  $\Sigma(t) = (\mathbf{Q}(t), \mathbf{Y}(t))$  denote the queue backlogs, we write the conditional Lyapunov drift-plus-penalty for slot  $t$  as

$$\Delta(\Sigma(t)) = \mathbb{E}[L(\Sigma(t+1)) - L(\Sigma(t)) | \Sigma(t)] - \nu U_0(\bar{\boldsymbol{\varphi}}), \quad (13)$$

where  $L(\Sigma(t)) \triangleq \frac{1}{2} \left[ \sum_{f=1}^F \sum_{b=0}^B Q_b^f(t)^2 + \sum_{f=1}^F Y_0^f(t)^2 \right]$  is the quadratic Lyapunov function of  $\Sigma(t)$  [12]. Here,  $\nu$  is a control parameter to trade off utility optimality and queue length. Note that the stability of  $\Sigma(t)$  assures that the constraints of problem (5c) and (11b) are held. Subsequently, following the straightforward calculations of the Lyapunov optimization, we obtain

$$\begin{aligned} (13) \leq \sum_{f=1}^F \sum_{b=1}^B \sum_m \pi_f^m z_f^m Q_b^f \left( R_{(b^{(1)}, b)}^f - R_{(b, b_f^{(o)})}^f \right) \\ - \sum_{f=1}^F \sum_{m=1, b_f^{(o)} \in \mathcal{Z}_f^m} \pi_f^m z_f^m Q_b^f R_{(b, b_f^{(o)})}^f \Big|_{b=0} \\ + \sum_{f=1}^F \left[ Y_0^f \varphi_0^f - \nu U(\varphi_0^f) - Y_0^f x_0^f \right] + \Psi. \end{aligned} \quad (14)$$

Due to space limitation, we omit the details of the constant value  $\Psi$  since it does not influence the system performance [12]. The solution to (11) can be obtained by minimizing the upper bound in (14), in which we have three decoupled sub-problems as follows: The flow-split vector and the probability distribution are determined by

$$\begin{aligned} \text{SP1: } \min_{\boldsymbol{\pi}, \mathbf{z}} \quad & \sum_{f=1}^F \Xi_f \\ \text{subject to} \quad & (5e), \end{aligned}$$

where

$$\begin{aligned} \Xi_f = \quad & \sum_{b=1}^B \sum_m \pi_f^m z_f^m Q_b^f \left( R_{(b^{(1)}, b)}^f - R_{(b, b_f^{(o)})}^f \right) \\ & - \sum_{m=1, b_f^{(o)} \in \mathcal{Z}_f^m} \pi_f^m z_f^m Q_b^f R_{(b, b_f^{(o)})}^f \Big|_{b=0}. \end{aligned}$$

Then, we select the optimal auxiliary variables by solving the following convex optimization problem

$$\begin{aligned} \text{SP2: } \min_{\boldsymbol{\varphi} | \mathbf{z}} \quad & \sum_{f=1}^F \left[ Y_0^f \varphi_0^f - \nu U(\varphi_0^f) \right] \\ \text{subject to} \quad & \varphi_0^f(t) \geq 0, \forall f \in \mathcal{F}. \end{aligned}$$

Let  $\varphi_0^{f*}$  be the optimal solution obtained by the first order derivative of the objective function of SP2. Assuming a logarithmic utility function, we have  $\varphi_0^{f*}(t) = \max \left\{ \frac{\nu}{Y_0^f}, 0 \right\}$ . Finally, the rate allocation is obtained by solving

$$\begin{aligned} \text{SP3: } \min_{\mathbf{x}, \mathbf{p} | \mathbf{z}} \quad & \sum_{f=1}^F -Y_0^f x_0^f \\ \text{subject to} \quad & (1), (4), (9), (10). \end{aligned}$$

#### A. Route Selection

To select the optimal routes in SP1, we leverage regret reinforcement learning which exploits the historical system information such as queue state and channel state [17]. Here, the regret learning method results in maximizing the long-term utility for each flow.

We denote  $u_f^m = u_f(z_f^m, \mathbf{z}_f^{-m})$  as an utility function of flow  $f$  when using path  $m$ . The vector  $\mathbf{z}_f^{-m}$  denotes the flow-split vector excluding path  $m$ . The MBS chooses more than one path, from SP1, the utility gain of flow  $f$  is

$$u_f = \sum_m u_f^m = -\Xi_f.$$

To exploit the historical information, the MBS determines a flow-split vector for each flow  $f$  from  $\mathcal{Z}_f$  based on the PMF from the previous stage  $t-1$ , i.e.,

$$\boldsymbol{\pi}_f(t-1) = \left( \pi_f^1(t-1), \dots, \pi_f^{Z_f}(t-1) \right). \quad (15)$$

Here, we define  $\mathbf{r}_f(t) = (r_f^1(t), \dots, r_f^m(t) \dots, r_f^{Z_f}(t))$  as a regret vector of determining flow-split vector for flow  $f$ . The MBS selects the flow-split vector with highest regret in which the mixed-strategy probability is given as

$$\pi_f^m(t) = \frac{\left[ r_f^m(t) \right]^+}{\sum_{m' \in \mathcal{Z}_f} \left[ r_f^{m'}(t) \right]^+}. \quad (16)$$

Let  $\hat{\mathbf{r}}_f(t) = (\hat{r}_f^1(t), \dots, \hat{r}_f^m(t) \dots, \hat{r}_f^{Z_f}(t))$  be the estimated regret vector of flow  $f$ , we introduce the Boltzmann-Gibbs (BG) distribution,  $\beta_f^m(\hat{\mathbf{r}}_f(t))$  to capture the exploitation and exploration for efficient learning [7], given by

$$\begin{aligned} \beta_f^m(\hat{\mathbf{r}}_f(t)) = \operatorname{argmax}_{\boldsymbol{\pi}_f \in \Pi} \sum_{m \in \mathcal{Z}_f} \left[ \pi_f^m(t) \hat{r}_f^m(t) \right. \\ \left. - \kappa_f \pi_f^m(t) \ln(\pi_f^m(t)) \right], \end{aligned} \quad (17)$$

where the trade-off factor  $\kappa_f$  is used to balance between exploration and exploitation. If  $\kappa_b$  is small, the SCBS selects  $\mathbf{z}_b$  with highest payoff. For  $\kappa_b \rightarrow \infty$  all decisions have equal probability.

For a given set of  $\hat{\mathbf{r}}_f(t)$  and  $\kappa_f$ , we solve (17) to find the probability distribution in which the solution determining the disjoint routes for each flow  $f$  is given as

$$\beta_f^m(\hat{\mathbf{r}}_f(t)) = \frac{\exp \left( \frac{1}{\kappa_f} \left[ \hat{r}_f^m(t) \right]^+ \right)}{\sum_{m' \in \mathcal{Z}_f} \exp \left( \frac{1}{\kappa_f} \left[ \hat{r}_f^{m'}(t) \right]^+ \right)}. \quad (18)$$

We denote  $\hat{u}(t)$  as the estimated utility of flow  $f$  at time instant  $t$  with action  $\mathbf{z}_f$ , i.e.,  $\hat{u}_f(t) = (\hat{u}_f^1(t), \dots, \hat{u}_f^m(t) \dots, \hat{u}_f^{Z_f}(t))$ . Upon receiving the feedback,  $\tilde{u}_f(t)$  denotes the utility observed by flow  $f$ , i.e.,  $\tilde{u}_f(t) = u_f(t-1)$ . Finally, we propose the learning mechanism at each time instant  $t$  as follows.

**Learning procedure:** The estimates of the utility, regret, and probability distribution functions are performed, and are updated for all actions as follows:

$$\begin{cases} \hat{u}_f^m(t) = \hat{u}_f^m(t-1) + \xi_f(t) \mathbb{I}_{\{\mathbf{z}_f = \mathbf{z}_f^m\}} \left( \tilde{u}_f(t) - \hat{u}_f^m(t-1) \right), \\ \hat{r}_f^m(t) = \hat{r}_f^m(t-1) + \gamma_f(t) \left( \hat{u}_f^m(t) - \tilde{u}_f(t) - \hat{r}_f^m(t-1) \right), \\ \pi_f^m(t) = \pi_f^m(t-1) + \iota_f(t) \left( \beta_f^m(\hat{\mathbf{r}}_f(t)) - \pi_f^m(t-1) \right). \end{cases} \quad (19)$$

Here,  $\xi_f(t)$ ,  $\gamma_f(t)$ , and  $\iota_f(t)$  are the learning rates which are chosen to satisfy the convergence properties (please see [17] for more details and convergence proof). Based on the probability distribution as per (19), the MBS selects the flow-split vector for each flow  $f$  as defined in Section III.

#### B. Rate Allocation

Consider  $R_{(i,j)}^f = \log(1 + p_{(i,j)}^f |g_{(i,j)}(\mathbf{h})|^2)$  as the transmission rate, where the effective channel gain for mmWave channels can be modeled as  $g_{(i,j)}(\mathbf{h}) = \frac{\tilde{g}_{(i,j)}(\mathbf{h})}{1 + I_{\max}^f}$  [18]. Here,  $\tilde{g}_{(i,j)}(\mathbf{h})$  and  $I_{\max}^f$  denote the normalized channel gain and the maximum interference, respectively [4]. Denoting the left hand side (LHS) of (9) and (10) as  $D_b^f$  for simplicity, the optimal values of flow control  $\mathbf{x}$  and transmit power  $\mathbf{p}$  are found by minimizing

$$\min_{\mathbf{x}, \mathbf{p} | \mathbf{z}} \sum_{f=1}^F -Y_0^f x_0^f \quad (20a)$$

$$\text{subject to } 1 + p_{(0,0^f)}^f |g_{(0,0^f)}|^2 \geq e^{x_0^f}, \forall f \in \mathcal{F}, \quad (20b)$$

$$\frac{1 + p_{(b,b_f^f)}^f |g_{(b,b_f^f)}|^2}{1 + p_{(b^{(1)},b)}^f |g_{(b^{(1)},b)}|^2} \geq e^{D_b^f}, \forall b \in \mathcal{S}^f, f \in \mathcal{F}, \quad (20c)$$

$$\sum_{f \in \mathcal{F}} p_{(b,b_f^f)}^f \leq P_b^{\max}, \forall b \in \mathcal{B}, \forall f \in \mathcal{F}. \quad (20d)$$

The constraint (20c) is non-convex, and the LHS of (20c) is an affine-over-affine function, which is jointly convex w.r.t the corresponding variables [19], [13]. By exploiting the hidden convexity of the problem, we propose an iterative rate allocation based on the successive convex approximation method. In this regard, we introduce the slack variable  $y$  to (20c) and rewrite it as

$$\frac{2 + p_{(b,b_f^f)}^f |g_{(b,b_f^f)}|^2}{2} \geq \sqrt{y^2 + \left( \frac{p_{(b,b_f^f)}^f |g_{(b,b_f^f)}|^2}{2} \right)^2}, \quad (21)$$

$$\frac{y^2}{1 + p_{(b^{(1)},b)}^f |g_{(b^{(1)},b)}|^2} \geq e^{D_b^f}. \quad (22)$$

Here, the constraint (21) holds a form of the second-order cone inequalities [13], while the LHS of constraint (22) is a quadratic-over-affine function which is iteratively replaced by the first order to achieve a convex approximation as follow

$$\frac{2yy^{(l)}}{1 + p_{(b^{(1)},b)}^{f(l)} |g_{(b^{(1)},b)}|^2} - \frac{y^{(l)2} \left( 1 + p_{(b^{(1)},b)}^f |g_{(b^{(1)},b)}|^2 \right)}{\left( 1 + p_{(b^{(1)},b)}^{f(l)} |g_{(b^{(1)},b)}|^2 \right)^2}. \quad (23)$$

The superscript  $l$  denotes the  $l$ th iteration. Hence, we iteratively solve the approximated convex problem of (20) as **Algorithm 1** in which the approximated problem is given as

$$\min_{\mathbf{x}, \mathbf{p} | \mathbf{z}} \sum_{f=1}^F -Y_0^f x_0^f \quad (24)$$

subject to (4), (20b), (20d), (21), (23).

Finally, the information flow diagram of the learning-aided path selection and rate allocation approach is shown in Fig. 2, where the rate allocation is executed in a short-term period.

---

**Algorithm 1** Iterative rate allocation

---

Initialization: set  $l = 0$  and generate initial points  $y^{(l)}$ .  
**repeat**  
  Solve (24) with  $y^{(l)}$  to get the optimal value  $y^{(l)*}$ .  
  Update  $y^{(l+1)} := y^{(l)*}$ ;  $l := l + 1$ .  
**until** Convergence

---

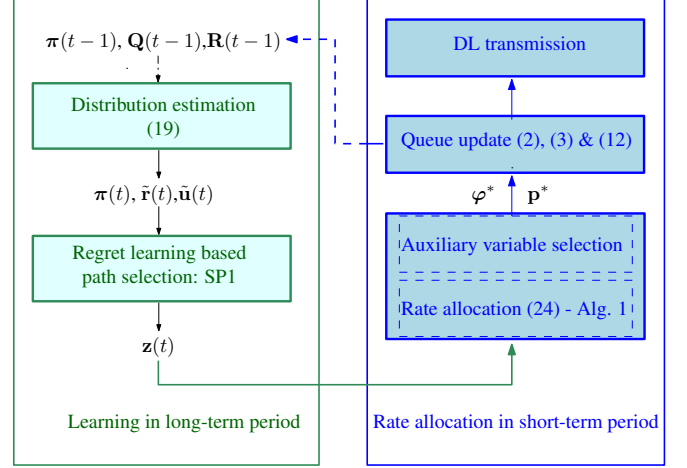


Fig. 2: Information flow diagram of the learning-aided path selection and rate allocation.

## V. NUMERICAL RESULTS

We provide numerical results by assuming two flows from the MBS to two UEs, while the number of available paths for each flow is four [10]. The MBS selects two routes from four most popular routes<sup>1</sup>. Each route contains two relays, the total number of SCBSs is 8, and the one-hop distance is varying from 50 to 100 meters. The maximum transmit power of MBS and each SCBS are 43 dBm and 30 dBm, respectively. The SCBS antenna gain is 5 dBi and the number of antennas at each BS is  $N_b = 8$ . We assume that the traffic flow is divided equally into two subflows, the arrival rate for each sub-flow is varying from 2 to 5 Gbps. The path loss is modeled as a distance-based path loss with the line-of-sight (LOS) model for urban environments at 28 GHz with 1 GHz of bandwidth [4]. The maximum delay requirement  $\beta$  and the target reliability probability  $\epsilon$  are set to be 10 ms and 0.05, respectively [5]. For the learning algorithm, the Boltzmann temperature  $\kappa_f$  is set to 5, while the learning rates  $\xi_f(t)$ ,  $\gamma_f(t)$ , and  $\iota_f(t)$  are set to  $\frac{1}{(t+1)^{0.5}}$ ,  $\frac{1}{(t+1)^{0.55}}$ , and  $\frac{1}{(t+1)^{0.6}}$ , respectively [17].

Furthermore, we compare our proposed scheme with the following baselines:

- **Baseline 1** considers a general NUM framework [12] with best path learning [17].
- **Baseline 2** considers a general NUM framework [12] and a random path section scheme, subject to (5b).
- **Baseline 3** considers a general NUM framework [12] and a random path section scheme.
- **Single hop** scheme: The MBS delivers data to UEs over one single hop at long distance in which the probability of LOS communication is low, and blockage is taken into account.

---

<sup>1</sup>As studied in [10], it suffices for a flow to maintain at least two paths provided that it repeatedly selects new paths at random and replaces if the latter provides higher throughput.

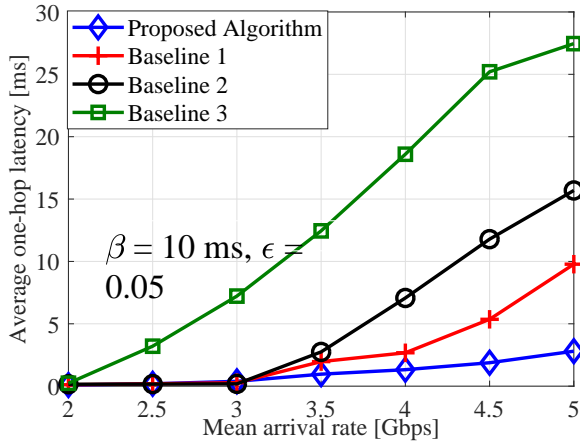


Fig. 3: Average one-hop delay versus mean arrival rates. In Fig. 3, we report the average one-hop delay<sup>2</sup> versus the mean arrival rates  $\bar{\mu}$ . As we increase  $\bar{\mu}$ , **baseline 3** violates the latency constraints, whereas our proposed algorithm outperforms the other **baselines**. The reason behind this gain is that the delay requirement is satisfied via the equivalent instantaneous rate by our proposed algorithm as per (9) and (10), while the **baselines 1** and **3** use the traditional utility-delay trade-off approach. Moreover, we apply the learning path algorithm, which selects the path with high payoff and less congestion resulting in small delay. The average one-hop delay of **baseline 1** with learning outperforms **baselines 2** and **3**, whereas our proposed scheme reduces latency by 50.64%, 81.32% and 92.9% as compared to **baselines 1, 2, and 3**, respectively, when  $\lambda = 4.5$  Gbps. When  $\lambda = 5$  Gbps, the average delay of all **baselines** increases, violating the delay requirement of 10 ms, while our proposed scheme is robust to the latency requirement. Moreover, for throughput comparison, we observe that for  $\lambda = 4.5$  Gbps, our proposed algorithm is able to deliver 4.4874 Gbps of average network throughput per each subflow, while the **baselines 1, 2, and 3** deliver 4.4759, 4.4682, and 4.3866 Gbps, respectively. Here, the **single hop** scheme only delivers 3.55 Gbps due to the blockage, which resulting in large delay.

In Fig. 4, we report the tail distribution (complementary cumulative distribution function (CCDF)) of latency to showcase how often the system achieves a delay greater than the target delay levels. In contrast to the average delay, the tail distribution is an important metric to reflect the URLLC characteristic. For instance, at  $\lambda = 4.5$  Gbps, by imposing the probabilistic latency constraint, our proposed approach ensures reliable communication with **better** guaranteed probability, i.e.,  $\Pr(\text{delay} > 10\text{ms}) < 10^{-6}$ . In contrast, **baseline 1** with learning violates the latency constraint with high probability, where  $\Pr(\text{delay} > 10\text{ms}) = 0.08$  and  $\Pr(\text{delay} > 25\text{ms}) < 10^{-6}$ , while the performance of **baselines 2 and 3** gets worse.

## VI. CONCLUSION

In this paper, we have proposed a multi-hop scheduling to support reliable communication by incorporating

<sup>2</sup>The average end-to-end delay can be defined as the sum of the average one-hop delay of all hops.

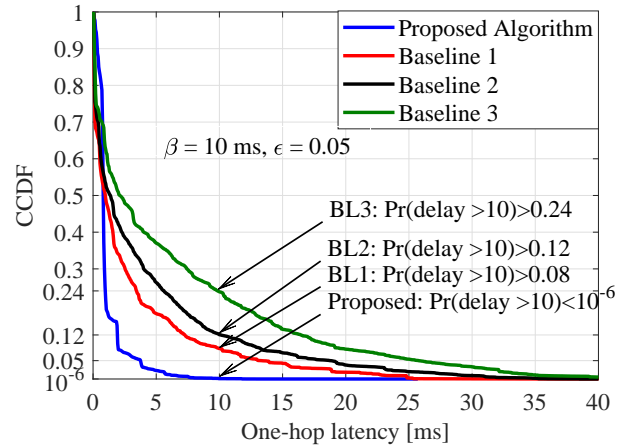


Fig. 4: CCDF of the one-hop latency,  $\bar{\mu} = 4.5$  Gbps.

the probabilistic latency constraint in 5G self-backhauled mmWave networks. In particular, the problem is modeled as a network utility maximization subject to a bounded latency constraint with a guaranteed probability, and queue stability. We have proposed a dynamic approach, which adapts to channel variations and system dynamics. We have leveraged stochastic optimization to decouple the studied problem into path selection and rate allocation sub-problems. Numerical results show that our proposed framework reduces latency by 50.64% and 92.9% as compared to **baselines**.

## ACKNOWLEDGMENT

The authors would like to thank Tekes, Nokia, Huawei, MediaTek, Keysight, Bittium and Kyynel for project funding. The Academy of Finland funding via the grant 307492 and the CARMA grants 294128 and 289611, the Nokia Foundation, and the Riitta and Jorma J. Takanen Foundation SR grant are also acknowledged.

## REFERENCES

- [1] J. G. Andrews et al., "What Will 5G Be?" *IEEE Journal on Selected Areas in Communications*, vol. 32, no. 6, pp. 1065–1082, June 2014.
- [2] T. S. Rappaport et al., "Millimeter wave mobile communications for 5G cellular: It will work!" *IEEE Access*, vol. 1, pp. 335–349, 2013.
- [3] A. Anpalagan, M. Bennis, and R. Vannithamby, *Design and Deployment of Small Cell Networks*. Cambridge University Press, 2015.
- [4] T. K. Vu, M. Bennis, S. Samarakoon, M. Debbah, and M. Latva-aho, "Joint load balancing and interference mitigation in 5G heterogeneous networks," *IEEE Transactions on Wireless Communications*, vol. 16, no. 9, pp. 6032–6046, Sep. 2017.
- [5] T. K. Vu, C.-F. Liu, M. Bennis, M. Debbah, M. Latva-aho, and C. S. Hong, "Ultra-reliable and low latency communication in mmwave-enabled massive MIMO networks," *IEEE Communications Letters*, vol. 21, no. 9, pp. 2041–2044, Sep. 2017.
- [6] S. Singh, F. Ziliotto, U. Madhow, E. Belding, and M. Rodwell, "Blockage and directivity in 60 GHz wireless personal area networks: From cross-layer model to multihop MAC design," *IEEE Journal on Selected Areas in Communications*, vol. 27, no. 8, 2009.
- [7] S. Samarakoon, M. Bennis, W. Saad, and M. Latva-aho, "Backhaul-aware interference management in the uplink of wireless small cell networks," *IEEE Transactions on Wireless Communications*, vol. 12, no. 11, pp. 5813–5825, 2013.
- [8] N. Eshraghi et al., "Millimeter-wave device-to-device multi-hop routing for multimedia applications," in *Proc. IEEE Int. Conf. Commun.*, Kuala Lumpur, Malaysia, May 2016, pp. 1–6.

- [9] B. Sahoo, C.-H. Yao, and H.-Y. Wei, "Millimeter-wave multi-hop wireless backhauling for 5g cellular networks," in *Proc. IEEE 85th Vehicular Technology Conf.*, Sydney, Australia, June 2017, pp. 1–6.
- [10] P. Key et al., "Path selection and multipath congestion control," in *Proc. the 26th IEEE Int. Conf. on Computer Communications (INFOCOM)*. Barcelona, Spain: IEEE, 2007, pp. 143–151.
- [11] M. Bennis, M. Debbah, and H. V. Poor, "Ultra-Reliable and Low-Latency Wireless Communication: Tail, Risk and Scale," *submitted to Proceedings of the IEEE*, 2018.
- [12] M. J. Neely, "Stochastic network optimization with application to communication and queueing systems," *Synthesis Lectures on Communication Networks*, vol. 3, no. 1, pp. 1–211, 2010.
- [13] S. Boyd and L. Vandenberghe, *Convex optimization*. Cambridge university press, 2004.
- [14] T. K. Vu, M. Bennis, S. Samarakoon, M. Debbah, and M. Latva-aho, "Joint in-band backhauling and interference mitigation in 5G heterogeneous networks," in *Proc. 22th European Wireless Conf.*, Oulu, Finland, May 2016, pp. 1–6.
- [15] A. Zakrzewska et al., "Dual connectivity in LTE HetNets with split control-and user-plane," in *Proc. IEEE Global Commun. Conf. Workshops*, Atlanta, GA, USA, Dec. 2013, pp. 391–396.
- [16] J. D. Little and S. C. Graves, "Little's law," in *Building intuition*. Springer, 2008, pp. 81–100.
- [17] M. Bennis, S. M. Perlaza, and M. Debbah, "Learning coarse correlated equilibria in two-tier wireless networks," in *Proc. IEEE Int. Conf. Commun.*, Ottawa, ON, Canada, Jun. 2012, pp. 1592–1596.
- [18] S. Hur et al., "Millimeter wave beamforming for wireless backhaul and access in small cell networks," *IEEE Trans. Commun.*, vol. 61, no. 10, pp. 4391–4403, Oct. 2013.
- [19] K. G. Nguyen et al., "Achieving energy efficiency fairness in multicell MISO downlink," *IEEE Communications Letters*, vol. 19, no. 8, pp. 1426–1429, 2015.